International Journal for Parasitology 42 (2012) 177–186

Contents lists available at SciVerse ScienceDirect

International Journal for Parasitology

journal homepage: www.elsevier.com/locate/ijpara

Dual targeting of aminoacyl-tRNA synthetases to the apicoplast and cytosol in *Plasmodium falciparum*

Katherine E. Jackson [a], James S. Pham [a], Michelle Kwek [a], Nilushi S. De Silva [a,1], Stacey M. Allen [a], Christopher D. Goodman [b], Geoffrey I. McFadden [b], Lluis Ribas de Pouplana [c,d], Stuart A. Ralph [a,*]

[a] *Department of Biochemistry and Molecular Biology, Bio21 Molecular Science and Biotechnology Institute, The University of Melbourne, Victoria 3010, Australia*
[b] *School of Botany, The University of Melbourne, Victoria 3010, Australia*
[c] *ICREA, Passeig Lluís Companys 1, Barcelona 08010, Catalonia, Spain*
[d] *Institute for Research in Biomedicine, Carrer Baldiri Reixac 10, Barcelona 08028, Catalonia, Spain*

ARTICLE INFO

Article history:
Received 24 October 2011
Received in revised form 22 November 2011
Accepted 23 November 2011
Available online 24 December 2011

Keywords:
Plasmodium
Malaria
Apicoplast
tRNA synthetase
Aminoacyl-tRNA synthetase
Dual targeting
Borrelidin
Mupirocin

ABSTRACT

The causative agent of malaria, *Plasmodium*, possesses three translationally active compartments: the cytosol, the mitochondrion and a relic plastid called the apicoplast. Aminoacyl-tRNA synthetases to charge tRNA are thus required for all three compartments. However, the *Plasmodium falciparum* genome encodes too few tRNA synthetases to supply a unique enzyme for each amino acid in all three compartments. We have investigated the subcellular localisation of three tRNA synthetases (AlaRS, GlyRS and ThrRS), which occur only once in the nuclear genome, and we show that each of these enzymes is dually localised to the *P. falciparum* cytosol and the apicoplast. No mitochondrial fraction is apparent for these three enzymes, which suggests that the *Plasmodium* mitochondrion lacks at least these three tRNA synthetases. The unique *Plasmodium* ThrRS is the presumed target of the antimalarial compound borrelidin. Borrelidin kills *P. falciparum* parasites quickly without the delayed death effect typical of apicoplast translation inhibitors and without an observable effect on apicoplast morphology. By contrast, mupirocin, an inhibitor of the apicoplast IleRS, kills with a delayed death effect that inhibits apicoplast growth and division. Because inhibition of dual targeted tRNA synthetases should arrest translation in all compartments of the parasite, these enzymes deserve further investigation as potential targets for antimalarial drug development.
Crown Copyright © 2012 Published by Elsevier Ltd. on behalf of Australian Society for Parasitology Inc. All rights reserved.

1. Introduction

Treatment of malaria is becoming increasingly complicated by the widespread resistance of *Plasmodium* parasites to many existing antimalarial drugs. This generates an intense and urgent need for development of new antimalarial drugs that are not compromised by existing resistance mechanisms. At least two antimalarial drugs, doxycycline and clindamycin, inhibit components of the protein translation machinery within the apicoplast (a relic plastid). The efficacy of these drugs validates protein translation as a key drug target in *Plasmodium*, and suggests other elements of the cytosolic or apicoplast protein translation machinery could act as potential targets for antimalarial compounds. One such family of enzymes involved in translation that has been advanced as promising drug targets is the aminoacyl-tRNA synthetase (aaRS) family. These enzymes are responsible for the charging of individual tRNA molecules with their cognate amino acids (Ibba and Soll, 2000; Ochsner et al., 2007). *Plasmodium*, like other eukaryotes, possesses organellar as well as cytosolic tRNA synthetases and several aaRS inhibitors inhibit growth of *Plasmodium* spp. The threonyl-tRNA synthetase inhibitor, borrelidin, potently kills *Plasmodium falciparum* parasites grown in culture (Ishiyama et al., 2011) and cures mice of rodent malaria infections (Otoguro et al., 2003). A clinically used inhibitor of bacterial type isoleucyl-tRNA synthetase, mupirocin (Ward and Campoli-Richards, 1986; Gurney and Thomas, 2011) and an inhibitor of the eukaryotic type isoleucyl-tRNA synthetase, thiaisoleucine, also inhibit growth of cultured *P. falciparum* (Istvan et al., 2011).

Inhibition of cytosolic protein machinery in *Plasmodium* generally leads to an immediate growth arrest, whereas inhibition of apicoplast-targeted protein machinery leads to a characteristic delayed death phenotype, where parasites do not die until the subsequent round of replication after treatment (Dahl and Rosenthal, 2007). Thiaisoleucine, an apparent inhibitor of the *Plasmodium* cytosolic IleRS, produced an immediate effect, whereas mupirocin,

* Corresponding author. Tel.: +61 3 8344 2284; fax: +61 3 9348 1421.
E-mail address: saralph@unimelb.edu.au (S.A. Ralph).
[1] Present address: Department of Microbiology & Immunology, Columbia University Medical Center, New York, NY 10032, USA.

0020-7519/$36.00 Crown Copyright © 2012 Published by Elsevier Ltd. on behalf of Australian Society for Parasitology Inc. All rights reserved.
doi:10.1016/j.ijpara.2011.11.008

an apparent inhibitor of the *Plasmodium* apicoplast IleRS, produced parasite growth inhibition consistent with the delayed death phenotype (Istvan et al., 2011). The action of the ThrRS inhibitor, borrelidin, against *Plasmodium* is at face value unusual because borrelidin kills parasites rapidly as would be expected for a cytosolic target enzyme, but the single ThrRS encoded by the *P. falciparum* genome (PF11_0270) (Bhatt et al., 2009; Jackson et al., 2011), starts with a very strongly-predicted apicoplast trafficking leader sequence (Foth et al., 2003). We therefore investigated the trafficking of this enzyme to study the nature of inhibition by borrelidin.

A distinct aaRS is needed to charge each tRNA with its cognate amino acid. Eukaryotic organelles such as plastids and mitochondria that have active translation machineries also require aaRS enzymes. Organellar genomes often encode all of their own tRNA molecules but all known aaRSs are nuclear encoded, so organellar aaRSs must be synthesised in the cytosol and post-translationally trafficked to their destination (Duchene et al., 2009). In numerous cases the demand for aaRS enzymes in the cytosol and in an organelle is met by dually targeting the same nuclear-encoded aaRS to both locations. Thus, for many aaRSs in *Saccharomyces cerevisiae*, a single nuclear gene encodes a protein that is localised to the cytosol as well as the mitochondria (Natsoulis et al., 1986; Chatton et al., 1988). In *Arabidopsis* the situation is even more complex, with some aaRS gene products being dually targeted to the chloroplast and the mitochondrion, and even some aaRSs that are found in the cytosol and both endosymbiotic organelles (Souciet et al., 1999; Duchene et al., 2005). Differential solubilisation experiments indicate that some aaRSs in the apicomplexan *Toxoplasma gondii* are also dually targeted to multiple compartments (Pino et al., 2009). The mechanisms for many of these multiple targeting events remain unclear.

We searched for possible examples of multiple targeted aaRSs encoded by *P. falciparum* genes (Gardner et al., 2002). As noted previously (Bhatt et al., 2009; Pino et al., 2009; Jackson et al., 2011), several aaRS proteins are found only once in the *Plasmodium* genome, including ThrRS (the presumed target of borrelidin), a predicted AlaRS and a predicted GlyRS. These are candidates for targeting to multiple compartments and allow us to specifically investigate whether the *Plasmodium* mitochondria harbours tRNA synthetases. No tRNA molecules are encoded by apicomplexan mitochondrial genomes and *Toxoplasma* appears to import tRNA from the cytosol (Esseiva et al., 2004; Pino et al., 2009). How these tRNAs are charged and recycled remains unknown. Here we dissect the trafficking of these three aaRS proteins (*Pf*AlaRS, *Pf*GlyRS and *Pf*ThrRS) using fluorescent protein and epitope tagging approaches, and demonstrate that each is dually targeted to the apicoplast and cytosol but not to the mitochondrion. We show that although the IleRS inhibitor, mupirocin, leads to a specific block in apicoplast division, borrelidin leads to an immediate growth arrest, consistent with inhibition of a *Pf*ThrRS that drives both cytosolic and apicoplast translation.

2. Materials and methods

2.1. Bioinformatic analysis

Sequences of the annotated *Pf*AlaRS (PF13_0354), *Pf*GlyRS (PF14_0198) and *Pf*Thr-RS (PF11_0270) were obtained from PlasmoDB (Aurrecoechea et al., 2009) (www.plasmodb.org). Sequences for putative orthologues were retrieved using BLAST searches (Altschul et al., 1997) of the GenBank non-redundant (nr) (Benson et al., 2011) and orthoMCL databases (Chen et al., 2006). Alignments were performed using ClustalW (Larkin et al., 2007). Analysis of the N-terminal targeting information was performed using SignalP (Bendtsen et al., 2004), PATS (Zuegge et al., 2001) and PlasmoAP (Foth et al., 2003), as well as through manual inspection of residues.

2.2. Parasite culture

Plasmodium falciparum parasites of the 3D7 strain were continuously cultured in O+ human erythrocytes (Australian Red Cross Blood Service, Melbourne, Australia) using a modification of the method established by Trager and Jensen (1976). *Plasmodium falciparum*-infected erythrocytes were maintained in RPMI-HEPES supplemented with 3.6% sodium bicarbonate and 5% Albumax (Invitrogen-Gibco, Australia). The cultures were incubated in an atmosphere of 5% CO_2, 1% O_2 and 94% N_2 at 37 °C. Parasite cultures were synchronised by repeatedly eliminating mature parasites using 5% sorbitol (Lambros and Vanderberg, 1979).

The double-transfectant *P. falciparum* parasites D10 ACP-RFP, CS-YFP were used to simultaneously image the mitochondria and apicoplast in live cells. This double transfectant stably expresses the apicoplast targeting sequence of acyl carrier protein (ACP) fused with red fluorescent protein (RFP) and the mitochondrial targeting sequence of citrate synthetase (CS) fused with yellow fluorescent protein (YFP) (van Dooren et al., 2005). The transfectant cell line was cultured as described above and under drug selection of 5 nM WR99210 and 2.5 μg/ml blasticidin S.

2.3. Drug assays

Parasite growth assays in response to drug treatment were conducted using the SYBR Green assay described by Smilkstein et al. (2004) with modifications as described by Goodman et al. (2007). The multi-drug resistant *P. falciparum* W2mef parasite strain was used for all drug assays. Growth was assayed after 48 h of drug treatment. For delayed death experiments, assays were also performed by treating parasites with inhibitor for 48 h, then replacing with media containing no inhibitor and growing a further 48 h before measuring growth. Compounds were dissolved in methanol, with a final methanol concentration of no greater than 0.1% in culture medium. Experiments were performed in triplicate and were independently performed at least three times.

D10 ACP-RFP, CS-YFP parasites were synchronised, then cultured in approximate 96-h IC_{90} concentrations of mupirocin (200 nM) and borrelidin (5.2 nM), or in 0.1% methanol carrier alone. Parasites were imaged 42 and 90 h after invasion.

2.4. Plasmids and transfection

A triple haemagglutinin (3× HA) tagging plasmid was used to tag the 3′ end of the endogenous copy of PF11_0270, PF13_0354 and PF14_0198 with a 3× HA repeat as previously described (Triglia et al., 2011). C-terminal fragments of PF11_0270 (855 bp), PF13_0354 (1124 bp) and PF14_0198 (849 bp) were amplified from *P. falciparum* 3D7 genomic DNA by PCR using the oligonucleotide pairs [5′gcggccgcGGATGCTCTATACGCAGCAAATG/5′ctgcagcAATGGTTTGGTTTGAGTTAAATTCC], [5′agatctCATCTAAGACGCATGAAGGAAATAATG/ctgcagcTTTGTTAATATTTTTAACATTTCTTCGGCATG] and [5′agatctGTTGGACATGCTGATAGATCAGC/ctgcagcGGAATCCAAAACCTGCTG], respectively. These fragments provide read-through of the native stop codons into the HA tags.

The PF11_0270 PCR fragment was cloned into the 3× HA-tagging plasmid with the *Not*I and *Pst*I sites and the PF13_0354 and PF14_0198 fragments were cloned using the *Bgl*II and *Pst*I sites. Ring stage *P. falciparum* of the 3D7 strain were transfected with 100 μg of purified plasmid DNA. Selection of stable integrants by 3′ single crossover recombination was performed as described by Duraisingh et al. (2002).

The pGlux plasmid was used to tag N-terminal fragments of PF11_0270, PF13_0354 and PF14_0198 with GFP as previously described (Boddey et al., 2009). The N-terminal fragments of PF11_0270 (1–180 bp), PF13_0354 (1–210 bp) and PF14_0198

(1–204 bp) were synthesised (Geneworks, Australia) with 5′*Xho*I and 3′*Xma*I restriction sites used to clone into the pGlux plasmid. Ring stage *P. falciparum* parasites of the 3D7 strain were transfected with 100 μg of purified plasmid DNA as described by Duraisingh et al. (2002) and grown in the presence of 5 nM WR99210.

2.5. Western blotting

Infected erythrocytes were tightly synchronised by treating twice with 5% sorbitol for 10 min at 37 °C, 18 h apart. Parasites were allowed to develop through trophozoite, schizont and ring stages where total protein from ring (8 h post-invasion), trophozoite (20 h post invasion) and schizont stages (40 h post invasion) was obtained by lysis with saponin 0.03% for 10 min at 4 °C in the presence of complete EDTA-free protease inhibitor (Roche, Australia). Proteins from 5×10^5 cells were separated on 3–8% Tris–Acetate gels with Tris–Acetate running buffer (Invitrogen). This loading corresponded to 9, 27 and 60 μg of total parasite protein for the ring, trophozoite and schizont samples, respectively. Proteins were transferred to Hybond polyvinylidene fluoride (PVDF) membrane (GE Healthcare Life Sciences, Australia) following standard western blotting protocols (Invitrogen, Australia). aaRS–HA fusions were identified with mouse anti-HA from Roche (1/1,000) followed by Molecular Probes anti-mouse HRP-conjugated IgG (1/5,000), while GFP fusions were labelled with mouse anti-GFP from Roche (1/1,000) followed by Molecular Probes anti-mouse HRP-conjugated IgG (1/5,000) and visualised using a chemiluminescence system (ECL, Pierce, Australia).

2.6. Immunofluorescence assays and microscopy

Erythrocytes infected with mixed stage parasites were fixed for 30 min at room temperature (RT) in PBS containing 4% (v/v) paraformaldehyde and 0.0075% (v/v) glutaraldehyde, washed in PBS, permeabilised with 0.1% (v/v) Triton X-100 in PBS for 10 min at RT and washed with PBS as described by Tonkin et al. (2004). Cells were incubated with 3% (w/v) BSA containing either rat anti-HA (1/100, Roche), mouse anti-HA (1/100, Roche), rabbit anti-ACP (1/500) or rabbit-anti-GFP (1/200, Roche) antibodies for 1 h at RT. Cells were washed in PBS and incubated in 3% (w/v) BSA containing Alexa Fluor 488-conjugated Goat anti-Rabbit/Rat/Mouse IgG (1:200, Molecular probes) for 1 h at RT. Finally, labelled cells were incubated with DAPI (0.5 μg/ml) for 5 min at RT, washed three times with PBS and mounted on a glass slide in the presence of DABCO mounting medium. Live cell imaging was conducted following incubation of infected erythrocytes with 20 nM of Mitotracker at 37 °C for 20 min and 0.5 μg/ml of DAPI for 5 min at RT.

To extract cytosol contents for viewing apicoplast labelling, parasites were treated with 0.2% saponin in PBS (compared with the 0.02–0.10% concentration that preserves plasma membrane integrity) prior to the fixation and preparation as described above.

Parasites were imaged with a Zeiss Axioplan2 using an AxioCamMR camera and AxioVision 4.5 software. Images shown were processed with ImageJ software (http://rsbweb.nih.gov/ij).

2.7. RNA extraction

Infected erythrocytes were tightly synchronised by treatment twice with 5% (w/v) sorbitol for 10 min at 37 °C, 18 h apart. Parasites were then allowed to develop through trophozoite, schizont and ring stages where mRNA from ring (8 h post-invasion) and schizont stages (40 h post invasion) was extracted using 10 vol. of TRIzol reagent (Invitrogen) for 10 min at 37 °C, followed by incubation with 0.2 TRIzol volumes of chloroform for 3 min at RT. Following centrifugation at 1,400*g* for 30 min at 4 °C the aqueous upper layer containing RNA was taken and RNA was precipitated with 0.5 TRIzol volumes of 2-propanol for at least 2 h at 4 °C. RNA was sedimented at 12,000*g* for 30 min at 4 °C. The RNA pellet was air-dried for 5 min and resuspended in 50 μl of formamide.

2.8. Digoxigenin (DIG)-probe synthesis

Specific probes for the identification of PF11_0270 (*Pf*ThrRS), PF13_0354 (*Pf*AlaRS) and PF14_0198 (*Pf*GlyRS) were amplified from *P. falciparum* 3D7 genomic DNA by PCR using the DIG probe synthesis kit (Roche) and the oligonucleotide pairs [5′gcggccgcGGATGCTCTATACGCAGCAAATG/5′ctgcagcAATGGTTTGGTTTGAGTTAAATTCC], [5′agatctCATCTAAGACGCATGAAGGAAATAATG/ctgcagcTTTGTTAATATTTTTAACATTTCTTCGGCATG] and [5′agatctGTTGGACATGCTGATAGATCAGC/ctgcagcGGAATCCAAAACCTGCTG], respectively, following the manufacturer's instructions.

2.9. Northern blotting

mRNA from 2×10^6 ring (8 h post-invasion) and schizont stage (40 h post invasion) parasites was denatured at 60 °C for 5 min, chilled on ice and separated through a 1.5% agarose gel prepared with TBE (89 mM Tris, 89 mM Borate and 2 mM EDTA, Ambion, Australia) and supplemented with 1× SYBRSafe (Invitrogen) and 1 M guanidine thiocynate (Sigma) at 5.5 V/cm for 15 min followed by 3.5 V/cm for 3 h. The gel was incubated twice in 7.5 mM NaOH (Sigma) for 15 min at RT and the RNA was transferred to Hybond N+ membrane overnight by capillary transfer following standard protocols. The membrane was neutralised in 2× SSC (0.3 M NaCl, 30 mM sodium citrate, pH 7), air-dried and UV cross-linked. The membrane was pre-hybridised in Church buffer (0.2 M NaH_2PO_4, 0.3 M Na_2HPO_4, 7% SDS) at 55 °C for 4 h. The membrane was hybridised with Church buffer containing denatured DIG-labelled specific probes (2 μl/ml) and herring sperm DNA (30 μg/ml) at 55 °C overnight. The membrane was washed in 0.5× SSC, 1% SDS prewarmed at 60 °C twice for 10 min. The detection of the DIG-labelled probes was performed using the DIG Nucleic Acid Detection kit (Roche) following the manufacturer's instructions for detection using enzyme-linked immunoassay with ready-to-use CSPD (chloro-5-substituted adamantyl-1,2-dioxetane phosphate, Roche, Australia).

2.10. Immunoprecipitation

Infected erythrocytes (~10% parasitemia in 2 ml packed erythrocytes) were lysed with saponin 0.03% for 10 min at 4 °C in the presence of complete EDTA-free protease inhibitors (Roche). Parasites were isolated by centrifugation at 5,000*g* for 5 min and washed three times in PBS. Cells were resuspended in 10 vol. of ice-cold TNET buffer (50 mM Tris, pH 7.4, 300 mM NaCl, 5 mM EDTA and 2% (w/v) Triton X-100) containing complete EDTA-free protease inhibitor and mixed by vortexing. Cells were incubated on ice for 30 min and vortexed three times. Soluble and insoluble material were separated by centrifugation at 16,000*g* for 20 min at 4 °C and the soluble fraction containing aaRSs was pre-cleared with protein A Sepharose (BioVision, Australia) for 1.5 h at 4 °C. The pre-cleared supernatant was incubated with mouse anti-HA (Roche)-conjugated protein A Sepharose for 4 h at 4 °C. The protein A Sepharose was washed three times in TNET and twice in PBS, both containing complete EDTA-free protease inhibitor (Roche). Immunoprecipitated pellets were combined with 30 μl 6× sample loading buffer and separated by SDS–PAGE through a 3–8% Tris–Acetate gels with Tris–Acetate running buffer (Invitrogen).

3. Results

3.1. Mupirocin inhibits apicoplast development but borrelidin leads to general cell-wide arrest

Two inhibitors of tRNA synthetases, mupirocin and borrelidin, have previously been shown to inhibit parasite growth (Otoguro et al., 2003; Ishiyama et al., 2011; Istvan et al., 2011). Mupirocin kills parasites with delayed death kinetics, consistent with apicoplast inhibition. We wished to directly compare the actions of mupriocin and borrelidin. We assayed parasites in the presence of serial dilutions of inhibitor, both by microscopic examination (Fig. 1A) and by SYBR green measurement of parasite nucleic acid (Smilkstein et al., 2004; Goodman et al., 2007). The concentrations of compound required to inhibit 50% of assayed growth (IC_{50}s) were determined for 48 h of treatment, as well as 48 h of treatment followed by an additional 48 h of growth with inhibitor washed out, in order to assay delayed death (Table 1). At 48 h mupirocin had only a minor effect at the highest concentrations tested (400 μM) but at 96 h the IC_{50} was 50 ± 4 nM S.D., comparable to the previously determined delayed death IC_{50} of 40.7 nM (assayed using a slightly different method) (Istvan et al., 2011). This confirms that mupirocin has no immediate killing effect, but does show potent delayed death. Borrelidin had a 48 h IC_{50} of 1.4 ± 0.2 nM S.D. but an only marginally lower 96 h IC_{50} of 1.25 nM ± 0.3 nM S.D., indicating that borrelidin does not have a delayed death phenotype. This 48 h IC_{50} is comparable to the published IC_{50} of borrelidin for *P. falciparum* strains K1 and FCR3 of 1.9 nM and 1.8 nm, respectively (Ishiyama et al., 2011).

We investigated the effect of these inhibitors on organelle morphology by growing parasites in the presence of IC_{90} concentrations of each compound for 92 h. Parasites with a RFP-labelled apicoplast and a YFP-labelled mitochondrion (D10 ACP-RFP, CS-YFP) were used to simultaneously visualise both organelles in live cells. Synchronised parasites were imaged at 40 h post invasion and at 92 h (i.e. second cycle) post invasion. Mupirocin treated parasites showed no apparent defect in the first cycle (40 h timepoint) but at 92 h apicoplast morphology was severely affected (Fig. 1B). While mitochondria continued to elongate and branch in these parasites, the apicoplast remained a single small punctum. Nuclear replication was also somewhat retarded. This effect has previously been observed with antibiotics that inhibit apicoplast translation (Dahl and Rosenthal, 2007). Borrelidin-treated parasites showed no such apicoplast-specific effect. Parasite growth was arrested by the 40 h timepoint and cells were visibly less healthy, but with no specific effect on mitochondrial or apicoplast branching or division (Fig. 1B). By 92 h many parasites had lysed but those few surviving parasites continued to show no specific organellar defect. Together, these data confirm the specific apicoplast effect of mupirocin, as shown by Istvan and colleagues (2011) but show that the effect of borrelidin is not restricted to an organelle-specific phenotype. This is inconsistent with the presumed target of borrelidin (*Pf*ThrRS) being restricted to the apicoplast.

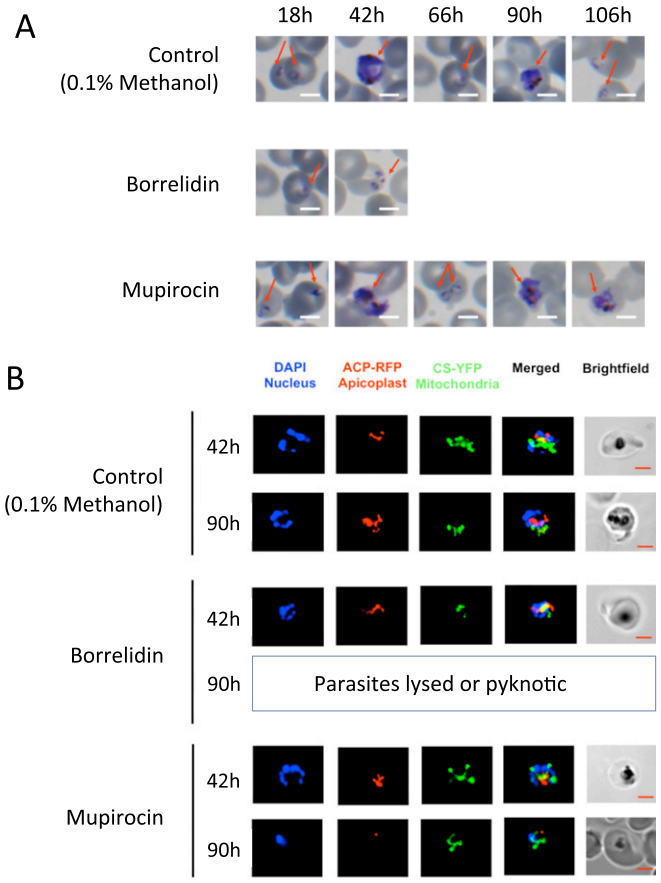

Fig. 1. Response of parasites to the aminoacyl-tRNA synthetase inhibitors borrelidin and mupirocin. (A) Synchronised parasites were treated at 18 h post invasion with concentrations of inhibitor at approximate IC_{90} concentrations; 200 nM mupirocin and 5.2 nM borrelidin, or with carrier alone – 0.1% methanol (control). Parasites (red arrows [grey in print version]) were analysed at the ring and schizont stages by light microscopy of Giemsa-stained smears. Borrelidin-treated parasites failed to develop into schizonts at 42 h, and the majority of parasites remained pyknotic without further development. Remnants of parasites were observed at 42 and 66 h. Mupirocin-treated parasites developed into normal schizonts at 42 h, produced merozoites that invaded red blood cells and formed rings, as observed at 66 h. The rings enlarged into dark trophozoites at 90 h. However, these parasites failed to develop into normal schizonts and did not produce additional merozoites, as observed at 106 h. This is characteristic of the delayed death phenotype, and is consistent with previous reports of mupirocin (Istvan et al., 2011). Scale bar = 4 μm. (B) Apicoplast division is inhibited by mupirocin but borrelidin leads to global cellular arrest. *Plasmodium* endosymbiotic organelles were visualised using double-transfected parasites with red fluorescent protein-labelled apicoplasts and yellow fluorescent protein-labelled mitochondria (D10 acyl carrier protein-RFP, citrate synthetase-YFP) (van Dooren et al., 2005). In the schizont stage of untreated parasites both the apicoplast and mitochondria elongate, branch and divide to segregate into daughter merozoites. In mupirocin-treated parasites (200 nM mupirocin), both organelles divided and segregated normally in the first round of treatment (42 h observation). However, after reinvading, parasites initially appeared normal, but apicoplasts did not elongate or branch, and no daughter merozoites were formed (90 h observation). Mitochondrial elongation and branching proceeded normally until schizont stages. In borrelidin-treated parasites, cells quickly (within 42 h) appeared shrunken and pyknotic, although no specific organellar defects were seen. Parasites did not proceed to make daughter merozoites. Some parasites persisted for another 48 h, but many were apparently lysed or pyknotic. Scale bar = 4 μm. (For interpretation of the references to colour in this figure legend, the reader is referred to the web version of this article.)

3.2. Plasmodium falciparum encodes single copies of AlaRS, GlyRS and ThrRS with predicted apicoplast targeting leader sequences

Bioinformatic analysis of the *P. falciparum* genome revealed only a single gene for each of AlaRS, GlyRS and ThrRS (Identifiers PF13_0354, PF14_0198 and PF11_0270, respectively). No aaRS genes were found in the apicoplast or mitochondrial genomes, and no significant hits to additional genes for these aaRS enzymes were discovered after extensive sequence similarity searching. Each of these three aaRS enzymes are highly conserved with the corresponding enzymes from other phyla. The *Pf*AlaRS is 46% identical/62% similar to the *Arabidopsis* AlaRS, the *Pf*GlyRS is 40% identical/58% similar to fungal GlyRSs and the *Pf*ThrRS is 49% identical/64% similar to fungal ThrRSs (Supplementary Fig. S1). Each of these three genes are single exon open reading frames (ORFs), although some very small introns in the untranslated regions (UTRs) of the *Pf*AlaRS are suggested by RNA-seq analysis (Bartfai et al., 2010). Se-

Table 1
Aminoacyl-tRNA synthetase inhibitor concentration to give 50% response (IC_{50}s) at 48 and 96 h.

	Borrelidin	Mupirocin
IC_{50} at 48 h	1.4 ± 0.2 nM	>400 μM
IC_{50} at 96 h	1.25 ± 0.3 nM	50 ± 4 nM

IC_{50}s as measured by SYBR Green assay (Smilkstein et al., 2004; Goodman et al., 2007) using *Plasmodium falciparum* W2Mef strain. Measurements were made after 48 h of drug treatment. After 48 h the parasites were washed in medium without drug and another measurement was made at 96 h. These data show that mupirocin, but not borrelidin, produces the delayed death phenotype.

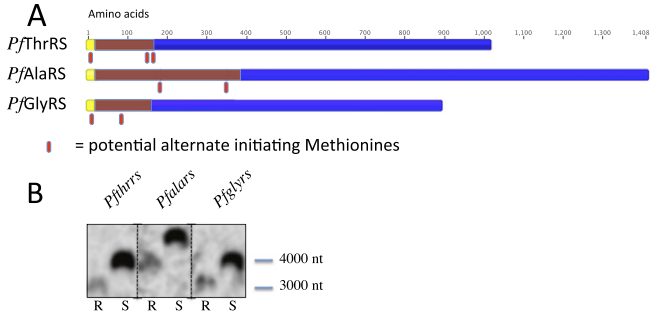

Fig. 2. Schematic of bioinformatic analysis of *Pf*ThrRS, *Pf*AlaRS and *Pf*GlyRS. (A) Each of these three unique *Plasmodium falciparum* (Pf) aminoacyl-tRNA synthetase-encoding genes encodes a product with a N-terminal extension that has no similarity to aaRSs outside the phylum Apicomplexa. This extension corresponds in each case to a predicted bipartite apicoplast leader that consists of a signal peptide followed by a transit peptide. In each case a methionine (conserved between *Plasmodium* spp. (Supplementary Fig. S1)) is positioned slightly upstream of the point at which the protein starts to match other aaRSs. Yellow (white in print version) signifies a signal sequence; and blue (dark grey in print version) signifies conservation with orthologues outside the phylum Apicomplexa. Red (light grey in print version) signifies potential alternate initiating methionines. Alignments showing sequence conservation are shown in Supplementary Fig. S1. (B) Northern blot analysis of *PfThrRS*, *PfAlaRS* and *PfGlyRS* mRNA. Northern blots reveal stage-specific differences in transcript length between ring stage (R) and schizont stage (S) parasites. Equal parasite numbers corresponding to 2×10^6 infected erythrocytes were loaded for each stage, then labelled with a probe specific for the 3′ end of the open reading frame for each of *pfthrrs*, *pfalars* and *pfglyrs*. For each of the three genes, a minor, shorter transcript species is observed in early ring parasites. nt, nucleotide. (For interpretation of the references to colour in this figure legend, the reader is referred to the web version of this article.)

quence analysis revealed the presence of a canonical N-terminal signal sequence (Fig. 2A) and each of *Pf*AlaRS-, *Pf*GlyRS- and *Pf*ThrRS were strongly predicted by PATS (Zuegge et al., 2001) and PlasmoAP (Foth et al., 2003) to be targeted to the apicoplast.

Alignment of *Plasmodium* AlaRS, GlyRS and ThrRS to their orthologues from other organisms revealed that each of these three aaRSs gene products contain N-terminal extensions ranging from approximately 100 amino acids as seen in *Pf*GlyRS to ~380 amino acids in the case of *Pf*AlaRS (Fig. 2A, Supplementary Fig. S1). These extensions are in each case predicted to contain apicoplast targeting information. How then might these genes encode isoforms of these proteins essential for the cytosol? One possible mechanism for dual targeting is alternate sites for initiation of translation, and each of these genes contains an internal methionine slightly N-terminal to the point at which the predicted proteins start showing substantial matches to their orthologues outside the phylum Apicomplexa (Met 350 for *Pf*AlaRS, Met 82 for *Pf*GlyRS, Met 150 for *Pf*ThrRS). Throughout the genus *Plasmodium*, this methionine is in the same position, or within a few residues, relative to the start of the matching enzyme sequence (Supplementary Fig. S1), consistent with a possible conserved function as an alternate initiation site.

3.3. Transcript analysis

Northern blotting was performed to explore the transcription of these genes in asexual parasite stages. Consistent with stage-specific RNA-seq analysis (Bartfai et al., 2010), these transcripts were considerably more abundant in schizont stages than in early ring stages (Fig. 2B). Unexpectedly, we observed a stage-specific difference in the size of the transcript for the three aaRSs, with all showing a short transcript in rings but a long transcript in schizont stage parasites (Fig. 2B). *Pf*AlaRS, which has a protein coding sequence of 4,227 nucleotides (nt), had a major band of approximately 5,000 nt in schizont stages, but a smaller band just over 4,000 nt in ring stages. *Pf*GlyRS, which has a protein coding sequence of 2,670 nt, showed a major transcript of approximately 4,000 nt in schizont stages but a shorter transcript of just over 3,000 nt in ring stages. *Pf*ThrRS, which has a protein coding sequence of 3,042 nt, also has a major transcript of approximately 4,000 nt in schizont stages but a shorter transcript of just over 3,000 nt in ring stages. No apparent introns are present in the coding regions, although some small introns are suggested by published RNA-seq data in the 5′UTR and 3′UTR of the *Pf*GlyRS (Bartfai et al., 2010). The differences in transcript lengths are thus likely to represent alternate transcript initiation or termination sites, which is consistent with available RNA-seq data for these genes (Bartfai et al., 2010).

3.4. The N-terminus of PfAlaRS, PfGlyRS and PfThrRS is sufficient for targeting GFP to the apicoplast in P. falciparum

We cloned N-terminal fragments of the *Pf*AlaRS (amino acids 1–70), *Pf*GlyRS (amino acids 1–68) and *Pf*ThrRS (amino acids 1–60) aaRS in front of GFP to determine whether these represent genuine apicoplast targeting leaders, as predicted by our bioinformatic analysis. These reporter fusions were transfected into the *P. falciparum* 3D7 strain and expressed episomally, transcribed using the *Pf*CRT promoter of the pGlux plasmid. Western blot analysis confirmed the expression of each of these fusion proteins in *P. falciparum* (Fig. 3C). Each of the three transfectant lines produced the characteristic doublet band with the upper band corresponding in size to an expected GFP fusion retaining an apicoplast transit peptide, and a second band around 4 kilodaltons (kDa) lower, which corresponds to a version with the transit peptide cleaved off. The upper bands run at approximate apparent masses of 33 kDa (*Pf*ThrRS), 33.5 kDa (*Pf*AlaRS) and 34 kDa (*Pf*GlyRS), consistent with their expected calculated masses of 32, 32.6 and 33 kDa, respectively (Fig. 3C). Signal peptides are co-translationally removed and we therefore do not expect to see a band representing such a full-length version. Apicoplast transit peptide cleavage sites are not well understood and can vary depending on fusion context, so we are unable to predict whether the transit peptide cleavage sites of these fusion proteins necessarily indicate the positions of transit peptide cleavage for the native proteins.

Live cell fluorescence of all three parasite lines showed clear localisation to an organelle reminiscent of the apicoplast (Fig. 3B). This signal was not found in the cytosol and did not colocalise with Mitotracker, a live cell stain for mitochondria (Fig. 3B). Colocalisation of anti-GFP labelling in immunofluorescence assays with a marker for the apicoplast (anti-ACP) confirmed that all three reporter fusions localise to the apicoplast (Fig. 3A). This confirms that the N-terminal extension of each of the these three aaRS gene products corresponds to an apicoplast-targeting sequence and does not direct protein targeting to the mitochondrion, nor to the cytosol.

3.5. HA-epitope tagging of PfAlaRS, PfGlyRS and PfThrRS

The localisation of genes through N-terminal fusion to GFP does not always provide the complete picture because only a fragment

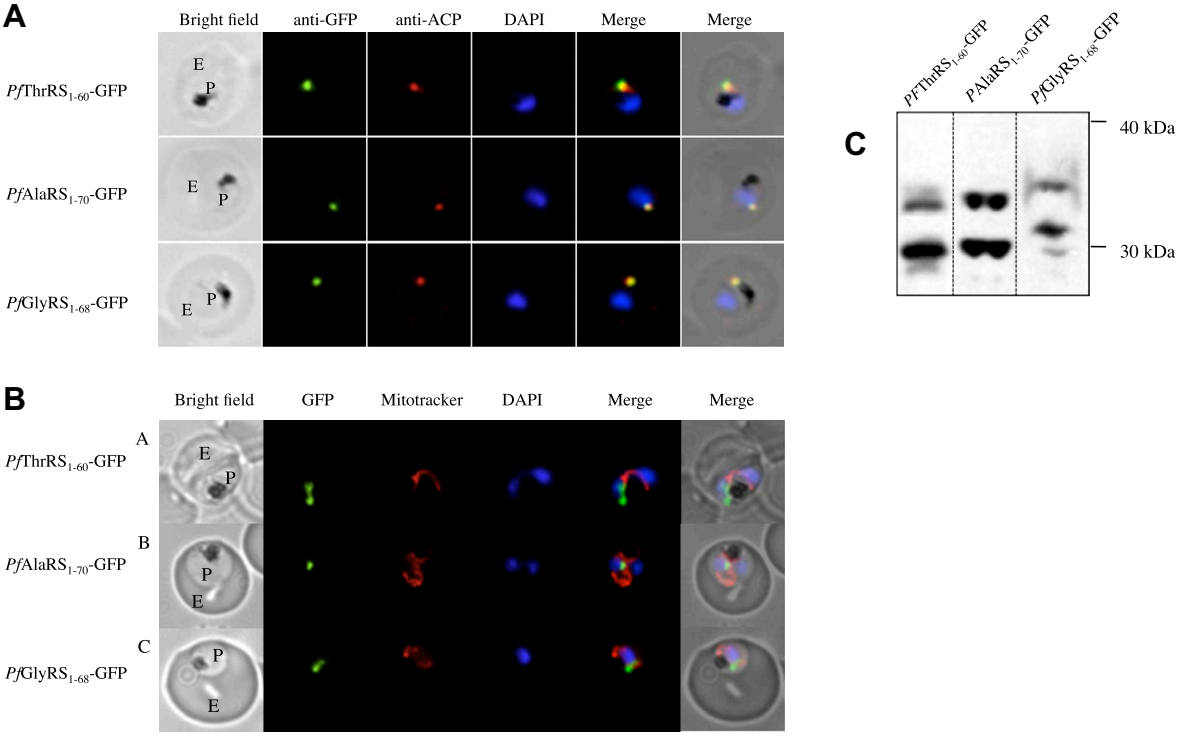

Fig. 3. The N-terminus of *Plasmodium falciparum* (*Pf*)ThrRS, *Pf*GlyRS and *Pf*AlaRS directs apicoplast targeting. (A) *Pf*ThrRS$_{1-60}$-GFP, *Pf*AlaRS$_{1-70}$-GFP and *Pf*GlyRS$_{1-68}$-GFP transfected parasites were labelled with anti-GFP and anti-acyl carrier protein antibodies and DAPI. The aminoacyl-tRNA synthetase–GFP fusions overlap with the apicoplast marker ACP, demonstrating that the N-terminus of these gene products is sufficient for apicoplast targeting. Bright field panels show the parasite (P) residing in its host erythrocyte (E). (B) Live cell microscopy shows that the N-terminal fragments of the aaRSs do not direct trafficking to mitochondria. Live parasites were stained using Mitotracker to highlight the mitochondria and this was compared with the GFP signal for each of the aaRS–GFP parasites. In all cases the mitochondria labelled a distinct and separate organelle from the GFP, indicating that these N-terminal leaders do not direct mitochondrial trafficking. (C) Western blotting (using anti-GFP antibody) of parasites transfected with the N-termini of the aaRS proteins fused to GFP shows that the apicoplast targeting leader is cleaved as expected. In each of the N-terminal aaRS–GFP fusions a doublet is seen corresponding to a longer version retaining the transit peptide (but lacking the co-translationally-removed signal peptide) and a shorter version with the transit peptide removed. A similar pattern is frequently observed with apicoplast-targeted proteins.

of the gene is used and because the transcript start site, transcription timing and transcript abundance are controlled by a heterologous promoter and chromatin context. We therefore further investigated the localisation of these tRNA synthetases through epitope tagging of the native chromosomal genes. Introduction of a C-terminal 3× HA tag by 3′ single crossover recombination allowed us to localise and follow the expression of the *Pf*AlaRS, *Pf*GlyRS and *Pf*ThrRS.

Western blotting confirmed that all three aaRSs were expressed at ring, trophozoite and schizont stages of *P. falciparum* development with maximal expression in the schizont stage (Fig. 4B). *Pf*ThrRS-HA migrated with an apparent molecular mass of just under 110 kDa (Fig. 4B), which is lower than the predicted molecular mass of 120 kDa for this protein lacking its predicted signal sequence, but consistent with translation initiation from the internal methionine at position 150 (expected mass 105 kDa). *Pf*AlaRS-HA migrated with an apparent molecular mass of just under 130 kDa (Fig. 4B), also significantly lower than its predicted molecular mass of 166 kDa for this protein lacking its predicted signal sequence, but consistent with initiation from the internal methionine at position 350 (predicted mass 127 kDa). *Pf*GlyRS-HA (Fig. 4) migrated with an apparent molecular mass of approximately 105 kDa, potentially consistent with a version at the full length (108 kDa), or with a version lacking the signal peptide (105 kDa), or even with a version initiating at methionine (98 kDa). Only a single specific band was observed for each of the HA-tagged aaRS proteins. Attempts to confirm the N-termini of these proteins by immunoprecipitating the proteins with anti-HA antibody, then analysing by MS/MS or Edman degradation, did not yield N-terminal peptide information.

3.6. HA-tagged PfAlaRS, PfGlyRS and PfThrRS are dual targeted to the parasite cytosol and apicoplast

Immunofluorescence assays performed on *Pf*AlaRS, *Pf*GlyRS and *Pf*ThrRS-HA transfectants revealed that in contrast to the clear uniquely-apicoplast localisation of the N-terminal GFP fusion, the dominant label for each of these proteins was located in the parasite cytosol (Fig. 4A). Colocalisation with the apicoplast marker ACP showed overlap with the smaller punctate apicoplasts, and in some cells there were foci of HA-labelling colocalising with the ACP-labelled apicoplast. Given the dominant fluorescence from the cytosolic fraction, it was not easy to discern whether the overlapping anti-HA signal was signal from adjacent cytosolic protein or a true apicoplast signal. The apicoplast is very narrow – as little as 200 nm wide – so is too small to robustly resolve whether a signal is adjacent to the apicoplast or within the lumen, even by three-dimensional confocal microscopy.

We therefore investigated selective permeabilisation methods to dissect the subcellular localisation of these HA tagged proteins. Saponin is routinely used to lyse erythrocyte membranes and parasite parasitophorous vacuole membranes at concentrations of between 0.02% and 0.1%, but at higher concentrations also lyses the parasite plasma membrane. Using antibodies against the apicoplast protein ACP to monitor apicoplast intactness, we examined parasites at high (0.1–0.5%) saponin concentrations. At 0.2% saponin, parasite plasma membranes were effectively permeabilised in most parasites allowing leaking of the cytosol, but apicoplasts were maintained as a single intact organelle. We therefore treated the HA-tagged parasites with 0.2% saponin to extract the dominant cytosolic signal. This treatment resulted in considerably less bright

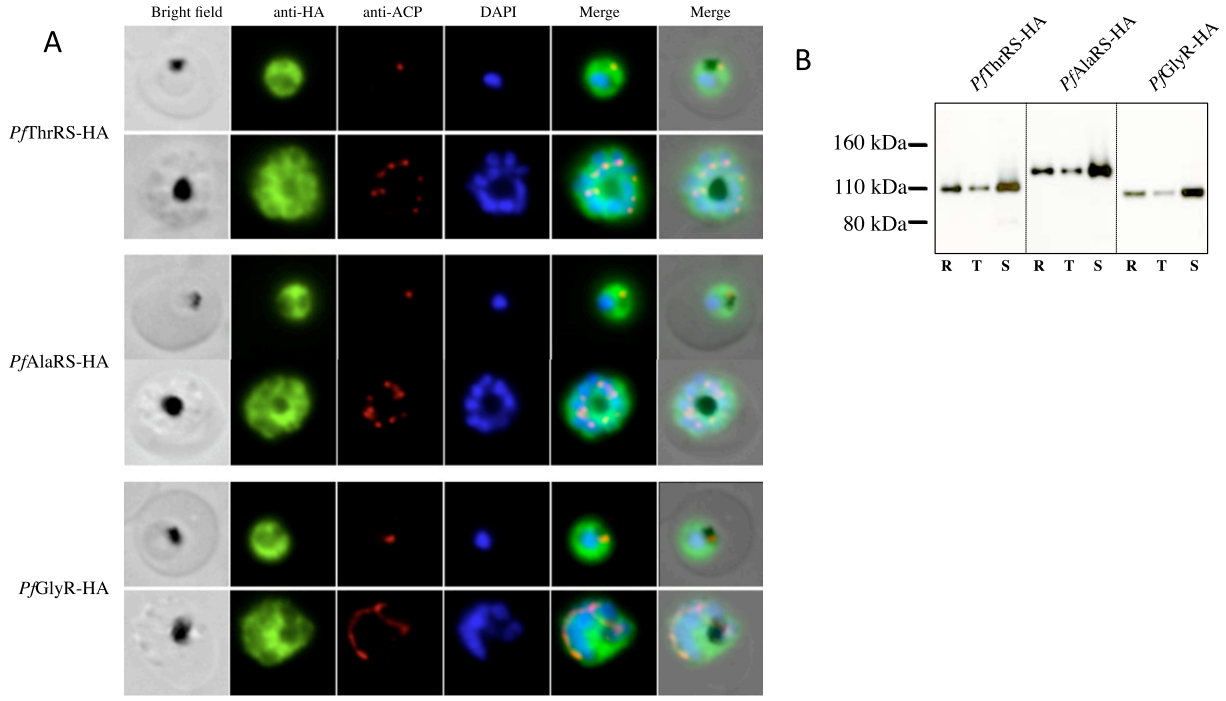

Fig. 4. Epitope-tagging of *Plasmodium falciparum* (*Pf*)ThrRS, *Pf*GlyRS and *Pf*AlaRS. (A) The single, chromosomal copies of *Pf*ThrRS, *Pf*GlyRS and *Pf*AlaRS were tagged with a triple hemagglutinin (3× HA) through transfection and 3′ replacement. Immunfluorescence assays show that the majority of each of these epitope tagged proteins is localised to the parasite cytosol. An early trophozoite and a schizont stage parasite are shown for each parasite line. Parasites were labelled with anti-HA and anti-acyl carrier protein antibodies and DAPI. Bright field panels show the parasite (P) residing in its host erythrocyte (E). Some epitope tagged protein colocalises with the apicoplast marker ACP, but the dominant signal from the cytosolic HA-tagged protein in these parasites makes it unclear whether this is specific colocalisation or signal from adjacent protein. The very small size of the apicoplast (~200 nm diameter) makes this question difficult to resolve by light microscopy under these conditions. (B) Western blot of 3× HA tagged *Pf*ThrRS, *Pf*GlyRS and *Pf*AlaRS. Equal parasite numbers were loaded for ring (R), trophozoite (T) and schizont (S) stages corresponding to 9, 27 and 60 μg of total protein, respectively. A single band is seen for each of the three aminoacyl-tRNA synthetase proteins. The mobility in each case corresponds to the mass of a protein initiating at the conserved internal methionines (Met 350 for AlaRS, Met 82 for GlyRS, Met 150 for ThrRS), suggesting that these dominant bands represent protein initiated at these alternate, internal methionines. This dominant protein fraction likely corresponds to the cytosolic product seen in A. No additional apicoplast product is observed in these parasites. It is not known whether the failure to detect a second product is because the apicoplast fraction is so minor in comparison to the cytosolic version – consistent with the immunofluorescence – or because the transit peptide cleavage site in these tagged native proteins is so close to the point of translation alternate initiation that the two are not electrophoretically separated.

fluorescence from the cytosol, and for each of the three HA-tagged aaRS proteins allowed clear visualisation of a residual punctum that colocalised with the apicoplast marker ACP (Fig. 5). A negative control using solely cytosolic GFP showed no overlap with the apicoplast in such preparations, nor did mismatched antibody controls, confirming the specificity of this localisation (data not shown). No adjacent labelling, potentially signifying mitochondrial localisation, was observed. These experiments therefore demonstrate that the HA-tagged *Pf*AlaRS, *Pf*GlyRS and *Pf*ThrRS are each dually targeted to the apicoplast and the cytosol. In each case the immunofluorescence assays showed that the great majority of the protein (we estimated well over 95% of the fluorescence) is found in the cytosol, but that a detectable fraction is specifically localised in the apicoplast when the cytosolic isoform is extracted.

All details of protein localisations have been submitted to ApiLoc (www.apiloc.biochem.unimelb.edu.au), a database for apicomplexan subcellular localisations.

4. Discussion

Our data indicate that *Plasmodium* provides for aminoacylation of apicoplast and cytosolic tRNA-Ala, tRNA-Gly and tRNA-Thr through the dual localisation of the three relevant aminoacyl-tRNA synthetases. Dual localisation of proteins is a widespread phenomenon, found in many if not all eukaryotes, and in a very high percentage of proteins within some species (Arnoys and Wang, 2007). In yeast, it is estimated that up to one-third of the mitochondrial proteome is also dually targeted to an additional compartment (Ben-Menachem et al., 2011). This phenomenon appears to be more common for some protein families than others, with proteins that can perform a useful function in multiple compartments being more likely to be recruited to diverse localisations. One such family is the aminoacyl-tRNA synthetases. Because these molecules are so ancient, and because their functions are frequently required in cytosol, mitochondria and plastids, there has been ample opportunity, and abundant examples, of the evolution of dual or even triple localisations of individual aaRSs (Duchene et al., 2005, 2009). In well-studied model organisms such as *S. cerevisiae* and *Arabidopsis thaliana*, many examples of the products of a single nuclear gene being targeted to two or more of the cytosol, mitochondria and plastid are known (Natsoulis et al., 1986; Chatton et al., 1988; Souciet et al., 1999; Duchene et al., 2005). Various molecular mechanisms have been proposed and demonstrated to achieve this alternate protein localisation.

A common mechanism for dual targeting of proteins is the production of alternately spliced transcripts that carry or lack targeting information (Takao et al., 1998; Lareau et al., 2004). An unusual example is the alternate trans-splicing of tRNA synthetases to produce alternately localised isoforms in *Trypanosoma brucei* (Rettig et al., in press). By contrast, an alternate cis-splicing mechanism apparently controls localisation of the *P. falciparum* protein MAEBL, where alternate splice forms either possess or lack a transmembrane domain, producing membrane-bound or soluble isoforms,

respectively (Singh et al., 2004). It is unclear whether alternate splicing has any role in the dual localisation of *Pf*AlaRS, *Pf*GlyRS or *Pf*ThrRS. Our northern blot data demonstrated that different transcripts for these genes exist in blood stage parasites and that these are regulated in a stage-specific manner (Fig. 2B). It is not known whether these transcript variants result from alternate splicing or the use of different transcription initiation or termination sites. RNA-seq data from other experiments (Bartfai et al., 2010; Otto et al., 2010) do not paint an entirely clear picture for these three genes, although in each case they are consistent with the northern data presented in Fig. 2. The *PfGlyRS* appears to have a transcript slightly over 3,000 nt in the early asexual stages, with some extension at the 3′ end seen in later stages, consistent with the size seen in the northern blot. Some small introns (~80–90 bp), with apparent slippage in 5′ and 3′ splice junction sites are also apparent in both the 5′UTR and 3′UTR of the *PfGlyRS* locus. The *PfAlaRS* locus has RNA-seq signal that indicates a product around 4,000 nt, in the earliest stages, as well as some slightly longer extensions at the 3′UTR in later stage parasites. The *PfThrRS* locus likewise has RNA-seq data indicating a product of just over 3,000 nt in early stages, as well as some extensions to this transcript at 5′ and 3′ ends in later stages (which may be separated by introns). The exact identity of these stage-variant transcripts certainly deserves further attention, potentially with reverse transcription-PCR methods including rapid amplification of 5′ cDNA ends (5′RACE) or oligo-dT-primed PCR to map the transcription initiation and termination sites.

Aside from alternate splicing or alternate transcriptional start sites, another way of producing multiple protein isoforms is through alternate translation initiation (Soldati et al., 1990; Fujino et al., 1997). In the case of *S. cerevisiae*, the ValRS and HisRS are targeted to both the cytosol and mitochondria as a result of two alternate translation initiation events leading to the generation of two aaRS isoforms: one with an N-terminal extension carrying mitochondrial targeting information and one without (Natsoulis et al., 1986; Chatton et al., 1988). This mechanism has also been suggested as the means of dual localisation for several *Plasmodium* proteins. A *P. falciparum* thioredoxin reductase (TxrR) is dually localised to the mitochondria and the cytosol, while a glutathione reductase seems to be localised to both the cytosol and apicoplast

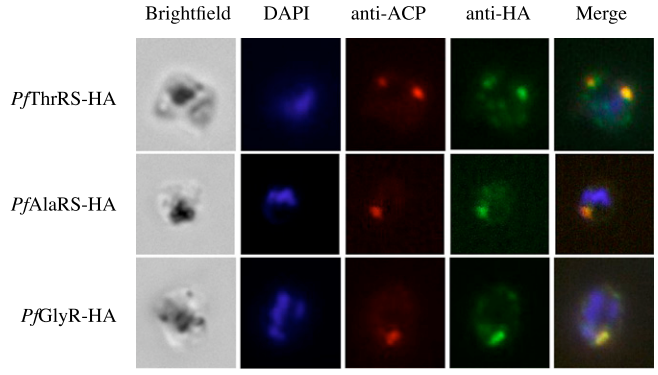

Fig. 5. Immuofluorescence assays of triple haemagglutinin (3× HA)-tagged *Plasmodium falciparum* aminoacyl-tRNA synthetase with cytosolic contents extracted demonstrate a residual fraction in the apicoplast. The major cytosolic fraction of the HA-tagged *Pf*AlaRS, *Pf*GlyRS and *Pf*ThrRS was extracted using 0.2% saponin incubation, a concentration that does not extract the apicoplast contents. In extracted parasites, a minor fraction of aaRS that colocalises with the acyl carrier protein-labelled apicoplast remains. These data demonstrate that although the majority of these 3× HA-tagged aaRS enzymes are resident in the cytosol, a minor fraction is specifically targeted to the apicoplast. Negative controls with solely cytosolic proteins, with secondary antibodies alone or with antibody swaps show no apicoplast localisation, confirming that the apicoplast localisation of the 3× HA-tagged *Pf*AlaRS, *Pf*GlyRS and *Pf*ThrRS is specific.

(Kehr et al., 2010). In both cases, the alternate subcellular localisations are likely to be due to alternate translation initiation (Kehr et al., 2010), where a full-length protein contains the organellar targeting sequence, but translation initiation from an internal methionine bypasses this trafficking leader and generates a cytosolic isoform. A mechanism of alternate translation initiation for the dual localised *Plasmodium* aaRSs is consistent with the western blot of the HA-tagged protein (Fig. 4B), and with the proteomic data available for these three proteins. For each of *Pf*AlaRS, *Pf*GlyRS and *Pf*ThrRS, abundant peptides have been detected in multiple proteomics experiments from various life stages (Florens et al., 2002; Lasonder et al., 2008; Bowyer et al., 2011). In all cases these peptides are detected downstream of the conserved internal methionine, which supports that this internal methionine is a major site for translation initiation. Another possible explanation for these data is that sequences N-terminal to this conserved internal methionine are translated and then rapidly cleaved and degraded. The western analysis of the HA-tagged aaRS proteins also suggests that most of the protein originates from these internal methionines, however we cannot exclude that the insertion of the HA-tagging sequence and *Plasmodium berghei* 3′UTR has perturbed the regulation of expression for this locus.

Another possible mechanism for alternate trafficking, observed in diverse proteins, is the use of a targeting sequence that is only inefficiently detected or bound by the protein sorting machinery, giving rise to one fraction of protein that is recognised and targeted to an organelle, while the remainder is retained in the cytosol or imported by another organelle (Peeters and Small, 2001). Dual targeting of aaRS to mitochondria and chloroplasts in plants appears to occur via an ambiguous N-terminal targeting peptide that is sloppily recognised by the import apparatus of both organelles (Berglund et al., 2009). Such a mechanism seems improbable for the characterised *Plasmodium* aaRS proteins, given that all of the GFP-reporter fused to the N-terminal of the aaRS was recognised and imported into the apicoplast (Fig. 3A). This indicates that when the N-termini of these proteins are present, they are efficiently recognised as apicoplast targeting sequences. We therefore favour a mechanism of alternate translation initiation mediating dual targeting of *Pf*AlaRS, *Pf*GlyRS and *Pf*ThrRS. This may either be connected to or independent from the apparent production of different transcripts for these genes. These phenomena warrant further studies to investigate if and how alternate translation initiation occurs, and to investigate the nucleic acid and protein elements of its regulation.

The reduction of an original three genes to satisfy aminoacylation of the apicoplast, mitochondrion and cytosol tRNAs to a single gene for each of Ala, Gly and Thr, prompts the question of the evolutionary origin of the retained gene. To address this, trees were constructed for each of the three aaRSs using multiple phylogenetic inference methods. The positions of the apicomplexan enzymes were poorly resolved, but for each of the three aaRSs studied, phylogenies show a clear eukaryotic origin, rather than derivation from the endosymbiont aaRSs that were presumably present in the ancestors of the apicoplast or the mitochondrion (data not shown). The evolutionary origins of these dually localised proteins can also be analysed by examining the situation in closely related apicomplexans. A different set of tRNA synthetases appear to be dual targeted in the apicomplexan parasite *T. gondii* (by mechanisms not yet understood) (Pino et al., 2009). Partial subcellular fractionation experiments suggest that at least *Toxoplasma* CysRS and perhaps ProRS are found in organellar as well as cytosolic fractions, while several other tRNA synthetases appear only once in the genome, so are likely candidates for dual localisation (Pino et al., 2009). It is noteworthy that all three of the *Plasmodium* enzymes investigated in this study, *Pf*AlaRS, *Pf*GlyRS and *Pf*ThrRS, are represented by two phylogenetically distinct genes in *T. gondii*

(Pino et al., 2009), so the evolution of dual targeting for these enzymes likely came after the split of haemosporidia from the coccidian parasites. AlaRS, GlyRS and ThrRS also appear only once in the genomes of closely related *Theileria* and *Babesia* parasites, so dual localisation of those proteins is probably shared in piroplasmida parasites. However, the gene models of these aaRSs in the sequenced piroplasmidae do not commence with predicted apicoplast targeting sequences, so it remains to be seen whether the mechanism of dual targeting for these genes is shared between these species.

One of the reasons that aaRSs can be successfully shared between organelles is that the substrates of these enzymes are relatively constant – ATP and the amino acids themselves look the same, irrespective of which compartment they inhabit. The exception of course is the tRNA molecule itself. Eukaryotic and bacterial tRNAs for the same amino acid can vary greatly at sequence and structural levels. So much so that bacterial tRNA synthetases frequently cannot recognise their cognate eukaryotic tRNAs, and conversely eukaryotic tRNA synthetases may not recognise bacterial tRNAs (Liu et al., 2011). The apicoplast encoded bacterial-type $tRNA^{Ala}$, $tRNA^{Gly}$ and $tRNA^{Thr}$ are highly diverged from the nuclear encoded eukaryotic-type equivalents, and the apicoplast encoded tRNAs are much more A + U rich than the nuclear encoded tRNAs (Preiser et al., 1995). Despite these differences, the dual targeting of single aaRSs responsible for charging both these sets of tRNAs strongly suggests that, for these tRNAs at least, the aaRS is able to recognise and charge both tRNA types. The translational responsibilities of the apicoplast are probably not onerous as the apicoplast genome encodes only a handful of proteins (Wilson et al., 1996), and its lumenal volume is small. The parasite may therefore be able to tolerate several eukaryotic aaRSs that efficiently recognise their eukaryotic tRNA substrates but can also charge the necessary apicoplast tRNAs with adequate capacity. These same unique tRNA synthetases must also be the enzymes responsible for charging the tRNAs used by the mitochondria. We find no evidence for these enzymes in mitochondria, so the charging must occur either in the cytosol or the apicoplast, followed by import of the charged tRNAs into the mitochondria. Nuclear encoded tRNAs have previously been detected in mitochondrial fractions of *T. gondii* in their aminoacylated forms (Esseiva et al., 2004; Pino et al., 2009), suggesting the mitochondrion uses nuclear tRNA charged in the cytosol. In addition, mitochondria persist in *P. falciparum* parasites that lack apicoplasts (Yeh and DeRisi, 2011), which indicates that it is the nucleus, rather than the apicoplast, that encodes the tRNA used by the mitochondria.

The elegant validation of the two *Plasmodium* IleRS enzymes as targets for several inhibitors (Istvan et al., 2011) already indicates that *Plasmodium* aaRSs are potential targets for drug development. Many other inhibitors are directed against a wide range of aaRSs from other organisms and these warrant further investigation in *Plasmodium*. Borrelidin is thought to inhibit ThrRS (Nass and Poralla, 1976; Otoguro et al., 2003), and our data indicate that this enzyme will be required for translation in all three translationally active compartments of *Plasmodium*. The immediacy of action of this compound, combined with its potential for wide ranging inhibition in the cell, makes the pursuit of further inhibitors of dual targeted *Plasmodium* aaRSs a worthy goal.

Acknowledgements

This work was funded by NHMRC (EU) Collaborative Research Grant 520700 in collaboration with the EU FP7 collaborative project Mephitis (HEALTH-F3-2009-223024) and a Program Grant from the NHMRC. SAR is funded by an Australian Research Council Future Fellowship FT0990350. JSP is funded by an Australian Postgraduate Award. GIM is a Federation Fellow of the Australian Research Council and a Howard Hughes International Scholar.

Appendix A. Supplementary data

Supplementary data associated with this article can be found, in the online version, at doi:10.1016/j.ijpara.2011.11.008.

References

Altschul, S.F., Madden, T.L., Schäffer, A.A., Zhang, J., Zhang, Z., Miller, W., Lipman, D.J., 1997. Gapped BLAST and PSI-BLAST: a new generation of protein database search programs. Nucleic Acids Res. 25, 3389–3402.

Arnoys, E.J., Wang, J.L., 2007. Dual localization: proteins in extracellular and intracellular compartments. Acta Histochem. 109, 89–110.

Aurrecoechea, C., Brestelli, J., Brunk, B.P., Dommer, J., Fischer, S., Gajria, B., Gao, X., Gingle, A., Grant, G., Harb, O.S., Heiges, M., Innamorato, F., Iodice, J., Kissinger, J.C., Kraemer, E., Li, W., Miller, J.A., Nayak, V., Pennington, C., Pinney, D.F., Roos, D.S., Ross, C., Stoeckert Jr., C.J., Treatman, C., Wang, H., 2009. PlasmoDB: a functional genomic database for malaria parasites. Nucleic Acids Res. 37, D539–D543.

Bartfai, R., Hoeijmakers, W.A., Salcedo-Amaya, A.M., Smits, A.H., Janssen-Megens, E., Kaan, A., Treeck, M., Gilberger, T.W., Francoijs, K.J., Stunnenberg, H.G., 2010. H2A.Z demarcates intergenic regions of the *Plasmodium falciparum* epigenome that are dynamically marked by H3K9ac and H3K4me3. PLoS Pathog. 6, e1001223.

Bendtsen, J.D., Nielsen, H., von Heijne, G., Brunak, S., 2004. Improved prediction of signal peptides: SignalP 3.0. J. Mol. Biol. 340, 783–795.

Ben-Menachem, R., Tal, M., Pines, O., 2011. A third of the yeast mitochondrial proteome is dual localized: a question of evolution. Proteomics 11, 4468–4476.

Benson, D.A., Karsch-Mizrachi, I., Lipman, D.J., Ostell, J., Sayers, E.W., 2011. GenBank. Nucleic Acids Res. 39, D32–D37.

Berglund, A.K., Pujol, C., Duchene, A.M., Glaser, E., 2009. Defining the determinants for dual targeting of amino acyl-tRNA synthetases to mitochondria and chloroplasts. J. Mol. Biol. 393, 803–814.

Bhatt, T.K., Kapil, C., Khan, S., Jairajpuri, M.A., Sharma, V., Santoni, D., Silvestrini, F., Pizzi, E., Sharma, A., 2009. A genomic glimpse of aminoacyl-tRNA synthetases in malaria parasite *Plasmodium falciparum*. BMC Genomics 10, 644.

Boddey, J.A., Moritz, R.L., Simpson, R.J., Cowman, A.F., 2009. Role of the *Plasmodium* export element in trafficking parasite proteins to the infected erythrocyte. Traffic 10, 285–299.

Bowyer, P.W., Simon, G.M., Cravatt, B.F., Bogyo, M., 2011. Global profiling of proteolysis during rupture of *Plasmodium falciparum* from the host erythrocyte. Mol. Cell. Proteomics 10, M110.001636.

Chatton, B., Walter, P., Ebel, J.P., Lacroute, F., Fasiolo, F., 1988. The yeast VAS1 gene encodes both mitochondrial and cytoplasmic valyl-tRNA synthetases. J. Biol. Chem. 263, 52–57.

Chen, F., Mackey, A.J., Stoeckert Jr., C.J., Roos, D.S., 2006. OrthoMCL-DB: querying a comprehensive multi-species collection of ortholog groups. Nucleic Acids Res. 34, D363–D368.

Dahl, E.L., Rosenthal, P.J., 2007. Multiple antibiotics exert delayed effects against the *Plasmodium falciparum* apicoplast. Antimicrob. Agents Chemother. 51, 3485–3490.

Duchene, A.M., Giritch, A., Hoffmann, B., Cognat, V., Lancelin, D., Peeters, N.M., Zaepfel, M., Marechal-Drouard, L., Small, I.D., 2005. Dual targeting is the rule for organellar aminoacyl-tRNA synthetases in *Arabidopsis thaliana*. Proc. Natl. Acad. Sci. U S A 102, 16484–16489.

Duchene, A.M., Pujol, C., Marechal-Drouard, L., 2009. Import of tRNAs and aminoacyl-tRNA synthetases into mitochondria. Curr. Genet. 55, 1–18.

Duraisingh, M.T., Triglia, T., Cowman, A.F., 2002. Negative selection of *Plasmodium falciparum* reveals targeted gene deletion by double crossover recombination. Int. J. Parasitol. 32, 81–89.

Esseiva, A.C., Naguleswaran, A., Hemphill, A., Schneider, A., 2004. Mitochondrial tRNA import in *Toxoplasma gondii*. J. Biol. Chem. 279, 42363–42368.

Florens, L., Washburn, M.P., Raine, J.D., Anthony, R.M., Grainger, M., Haynes, J.D., Moch, J.K., Muster, N., Sacci, J.B., Tabb, D.L., Witney, A.A., Wolters, D., Wu, Y., Gardner, M.J., Holder, A.A., Sinden, R.E., Yates, J.R., Carucci, D.J., 2002. A proteomic view of the *Plasmodium falciparum* life cycle. Nature 419, 520–526.

Foth, B.J., Ralph, S.A., Tonkin, C.J., Struck, N.S., Fraunholz, M., Roos, D.S., Cowman, A.F., McFadden, G.I., 2003. Dissecting apicoplast targeting in the malaria parasite *Plasmodium falciparum*. Science 299, 705–708.

Fujino, T., Man-Jong, K., Minekura, H., Suzuki, H., Yamamoto, T.T., 1997. Alternative translation initiation generates acyl-CoA synthetase 3 isoforms with heterogeneous amino termini. J. Biochem. 122, 212–216.

Gardner, M.J., Hall, N., Fung, E., White, O., Berriman, M., Hyman, R.W., Carlton, J.M., Pain, A., Nelson, K.E., Bowman, S., Paulsen, I.T., James, K., Eisen, J.A., Rutherford, K., Salzberg, S.L., Craig, A., Kyes, S., Chan, M.S., Nene, V., Shallom, S.J., Suh, B., Peterson, J., Angiuoli, S., Pertea, M., Allen, J., Selengut, J., Haft, D., Mather, M.W., Vaidya, A.B., Martin, D.M., Fairlamb, A.H., Fraunholz, M.J., Roos, D.S., Ralph, S.A., McFadden, G.I., Cummings, L.M., Subramanian, G.M., Mungall, C., Venter, J.C., Carucci, D.J., Hoffman, S.L., Newbold, C., Davis, R.W., Fraser, C.M., Barrell, B., 2002. Genome sequence of the human malaria parasite *Plasmodium falciparum*. Nature 419, 498–511.

Goodman, C.D., Su, V., McFadden, G.I., 2007. The effects of anti-bacterials on the malaria parasite *Plasmodium falciparum*. Mol. Biochem. Parasitol. 152, 181–191.

Gurney, R., Thomas, C.M., 2011. Mupirocin: biosynthesis, special features and applications of an antibiotic from a gram-negative bacterium. Appl. Microbiol. Biotechnol. 90, 11–21.

Ibba, M., Soll, D., 2000. Aminoacyl-tRNA synthesis. Annu. Rev. Biochem. 69, 617–650.

Ishiyama, A., Iwatsuki, M., Namatame, M., Nishihara-Tsukashima, A., Sunazuka, T., Takahashi, Y., Omura, S., Otoguro, K., 2011. Borrelidin, a potent antimalarial: stage-specific inhibition profile of synchronized cultures of *Plasmodium falciparum*. J. Antibiot. (Tokyo) 64, 381–384.

Istvan, E.S., Dharia, N.V., Bopp, S.E., Gluzman, I., Winzeler, E.A., Goldberg, D.E., 2011. Validation of isoleucine utilization targets in *Plasmodium falciparum*. Proc. Natl. Acad. Sci. U S A 108, 1627–1632.

Jackson, K.E., Habib, S., Frugier, M., Hoen, R., Khan, S., Pham, J.S., Pouplana, L.R., Royo, M., Santos, M.A., Sharma, A., Ralph, S.A., 2011. Protein translation in *Plasmodium* parasites. Trends Parasitol. 27, 467–476.

Kehr, S., Sturm, N., Rahlfs, S., Przyborski, J.M., Becker, K., 2010. Compartmentation of redox metabolism in malaria parasites. PLoS Pathog. 6, e1001242.

Lambros, C., Vanderberg, J.P., 1979. Synchronization of *Plasmodium falciparum* erythrocytic stages in culture. J. Parasitol. 65, 418–420.

Lareau, L.F., Green, R.E., Bhatnagar, R.S., Brenner, S.E., 2004. The evolving roles of alternative splicing. Curr. Opin. Struct. Biol. 14, 273–282.

Larkin, M.A., Blackshields, G., Brown, N.P., Chenna, R., McGettigan, P.A., McWilliam, H., Valentin, F., Wallace, I.M., Wilm, A., Lopez, R., Thompson, J.D., Gibson, T.J., Higgins, D.G., 2007. Clustal W and Clustal X version 2.0. Bioinformatics 23, 2947–2948.

Lasonder, E., Janse, C.J., van Gemert, G.J., Mair, G.R., Vermunt, A.M.W., Douradinha, B.G., van Noort, V., Huynen, M.A., Luty, A.J.F., Kroeze, H., Khan, S.M., Sauerwein, R.W., Waters, A.P., Mann, M., Stunnenberg, H.G., 2008. Proteomic profiling of Plasmodium sporozoite maturation identifies new proteins essential for parasite development and infectivity. PLoS Pathog 4, e1000195.

Liu, C., Gamper, H., Liu, H., Cooperman, B.S., Hou, Y.M., 2011. Potential for interdependent development of tRNA determinants for aminoacylation and ribosome decoding. Nat. Commun. 2, 329.

Nass, G., Poralla, K., 1976. Genetics of borrelidin resistant mutants of *Saccharomyces cerivisiae* and properties of their threonyl-tRNA-synthetase. Mol. Gen. Genet. 147, 39–43.

Natsoulis, G., Hilger, F., Fink, G.R., 1986. The HTS1 gene encodes both the cytoplasmic and mitochondrial histidine tRNA synthetases of *S. cerevisiae*. Cell 46, 235–243.

Ochsner, U.A., Sun, X., Jarvis, T., Critchley, I., Janjic, N., 2007. Aminoacyl-tRNA synthetases: essential and still promising targets for new anti-infective agents. Expert Opin. Investig. Drugs 16, 573–593.

Otoguro, K., Ui, H., Ishiyama, A., Kobayashi, M., Togashi, H., Takahashi, Y., Masuma, R., Tanaka, H., Tomoda, H., Yamada, H., Omura, S., 2003. In vitro and in vivo antimalarial activities of a non-glycosidic 18-membered macrolide antibiotic, borrelidin, against drug-resistant strains of Plasmodia. J. Antibiot. (Tokyo) 56, 727–729.

Otto, T.D., Wilinski, D., Assefa, S., Keane, T.M., Sarry, L.R., Bohme, U., Lemieux, J., Barrell, B., Pain, A., Berriman, M., Newbold, C., Llinas, M., 2010. New insights into the blood-stage transcriptome of *Plasmodium falciparum* using RNA-Seq. Mol. Microbiol. 76, 12–24.

Peeters, N., Small, I., 2001. Dual targeting to mitochondria and chloroplasts. Biochim. Biophys. Acta 1541, 54–63.

Pino, P., Aeby, E., Foth, B.J., Sheiner, L., Soldati, T., Schneider, A., Soldati-Favre, D., 2009. Mitochondrial translation in absence of local tRNA aminoacylation and methionyl tRNA Met formylation in Apicomplexa. Mol. Microbiol. 76, 706–718.

Preiser, P., Williamson, D.H., Wilson, R.J.M., 1995. TRNA genes transcribed from the plastid-like DNA of *Plasmodium falciparum*. Nucleic Acids Res. 23, 4329–4336.

Rettig, J., Wang, Y., Schneider, A., Ochsenreiter, T., in press. Dual targeting of isoleucyl-tRNA synthetase in *Trypanosoma brucei* is mediated through alternative trans-splicing. Nucleic Acids Res. doi:10.1093/nar/gkr794.

Singh, N., Preiser, P., Renia, L., Balu, B., Barnwell, J., Blair, P., Jarra, W., Voza, T., Landau, I., Adams, J.H., 2004. Conservation and developmental control of alternative splicing in maebl among malaria parasites. J. Mol. Biol. 343, 589–599.

Smilkstein, M., Sriwilaijaroen, N., Kelly, J.X., Wilairat, P., Riscoe, M., 2004. Simple and inexpensive fluorescence-based technique for high-throughput antimalarial drug screening. Antimicrob. Agents Chemother. 48, 1803–1806.

Soldati, T., Schafer, B.W., Perriard, J.C., 1990. Alternative ribosomal initiation gives rise to chicken brain-type creatine kinase isoproteins with heterogeneous amino termini. J. Biol. Chem. 265, 4498–4506.

Souciet, G., Menand, B., Ovesna, J., Cosset, A., Dietrich, A., Wintz, H., 1999. Characterization of two bifunctional *Arabdopsis thaliana* genes coding for mitochondrial and cytosolic forms of valyl-tRNA synthetase and threonyl-tRNA synthetase by alternative use of two in-frame AUGs. Eur. J. Biochem. 266, 848–854.

Takao, M., Aburatani, H., Kobayashi, K., Yasui, A., 1998. Mitochondrial targeting of human DNA glycosylases for repair of oxidative DNA damage. Nucleic Acids Res. 26, 2917–2922.

Tonkin, C.J., van Dooren, G.G., Spurck, T.P., Struck, N.S., Good, R.T., Handman, E., Cowman, A.F., McFadden, G.I., 2004. Localization of organellar proteins in *Plasmodium falciparum* using a novel set of transfection vectors and a new immunofluorescence fixation method. Mol. Biochem. Parasitol. 137, 13–21.

Trager, W., Jensen, J., 1976. Human malaria parasites in continuous culture. Science 193, 673–675.

Triglia, T., Chen, L., Lopaticki, S., Dekiwadia, C., Riglar, D.T., Hodder, A.N., Ralph, S.A., Baum, J., Cowman, A.F., 2011. *Plasmodium falciparum* merozoite invasion is inhibited by antibodies that target the PfRh2a and b binding domains. PLoS Pathog. 7, e1002075.

van Dooren, G.G., Marti, M., Tonkin, C.J., Stimmler, L.M., Cowman, A.F., McFadden, G.I., 2005. Development of the endoplasmic reticulum, mitochondrion and apicoplast during the asexual life cycle of *Plasmodium falciparum*. Mol. Microbiol. 57, 405–419.

Ward, A., Campoli-Richards, D.M., 1986. Mupirocin: a review of its antibacterial activity, pharmacokinetic properties and therapeutic use. Drugs 32, 425–444.

Wilson, R.J.M., Denny, P.W., Preiser, P.R., Rangachari, K., Roberts, K., Roy, A., Whyte, A., Strath, M., Moore, D.J., Moore, P.W., Williamson, D.H., 1996. Complete gene map of the plastid-like DNA of the malaria parasite *Plasmodium falciparum*. J. Mol. Biol. 261, 155–172.

Yeh, E., DeRisi, J.L., 2011. Chemical rescue of malaria parasites lacking an apicoplast defines organelle function in blood-stage *Plasmodium falciparum*. PLoS Biol. 9, e1001138.

Zuegge, J., Ralph, S., Schmuker, M., McFadden, G.I., Schneider, G., 2001. Deciphering apicoplast targeting signals – feature extraction from nuclear-encoded precursors of *Plasmodium falciparum* apicoplast proteins. Gene 280, 19–26.